Analysis of the Structure of Ribonuclease A in Native and Partially Denatured States by Time-Resolved Nonradiative Dynamic Excitation Energy Transfer between Site-Specific Extrinsic Probes†

David R. Buckler,‡,§ Elisha Haas,‖ and Harold A. Scheraga*,‡

Baker Laboratory of Chemistry, Cornell University, Ithaca, New York 14853-1301, and Department of Life Sciences, Bar-Ilan University, Ramat-Gan 52900, Israel

Received April 3, 1995; Revised Manuscript Received September 21, 1995⊗

ABSTRACT: Formation of local structure and overall chain dimensions in the 124-residue, four-disulfide protein bovine pancreatic ribonuclease A (RNase A) under conditions favoring either the native or partially folded states have been studied by nonradiative excitation energy transfer measurements. Three RNase A derivatives, doubly labeled with 2-naphthylalanine amide (fluorescent donor) at the C-terminus of each and 7-carboxymethylamino-4-methyl-coumarin (fluorescent acceptor) at the ϵ-amino group of lysine 1, 61, and 104, respectively [(1−124)RNase A, (61−124)RNase A, and (104−124)RNase A], were prepared. RNase A was modified by a two-step labeling strategy involving prior modification of the C-terminus with the donor probe by enzymatic methods, followed by modification of lysine ϵ-amino groups with the coumarin derivative. The derivatives were purified by liquid chromatography and characterized by tryptic mapping. The mono-labeled donor derivative (without acceptor) undergoes a reversible thermal folding transition (T_m = 48.3 °C; native RNase A, T_m= 54.4 °C), and all labeled derivatives retain enzymatic activity (activities against the substrate cCMP relative to native are 87 ± 5%, 94 ± 6.5%, 79 ± 10%, and 207 ± 15% for the donor-only and doubly-labeled derivatives with the acceptor at Lys 104, 61, and 1, respectively), supporting the suitability of these derivatives for protein folding studies. Time-resolved fluorescence measurements were used to determine the extent of nonradiative excitation energy transfer between donor and acceptor probes, which allowed recovery of parameters describing the distribution of interprobe distances and the diffusion coefficient of the ends of the segments defined by the pairs of sites labeled by the probes. Use of a donor with a relatively long intrinsic fluorescence decay rate allowed greater precision in the recovery of the interprobe diffusion coefficients compared with earlier studies using donors with shorter intrinsic decay rates, and this parameter provides an important measure of the extent of folding and degree of packing of the chain segments. Analyses for each derivative were carried out under solution conditions favoring native (pH 5.0, 22 °C, <0.7 M guanidinium hydrochloride) or denatured (>6 M guanidinium hydrochloride) chain conformations, both with and without intact disulfide bonds (in the absence or presence of dithiothreitol, respectively). For (1−124)RNase A in the native state, high interprobe diffusion rates and a broad interprobe distance distribution suggest flexibility of the N-terminal segment, in the native state in solution, that is not observed in the same segment of the unmodified molecule in the crystalline state analyzed by X-ray diffraction. At high (>6 M) guanidinium hydrochloride concentration in solution, addition of DTT resulted in an expected increase of the mean EED of the 64-residue segment in (61−124)RNase A, as a result of disulfide bond cleavage. The transfer of the molecule from high to low denaturant concentration with disulfides broken resulted in a contraction of overall chain dimensions [the EED decreased from 33.3 Å to 22 Å for the (104−124) segment and from >50 Å to 38 Å for the (61−124) segment as a result of this transfer]. In conclusion, the measurements show that the unfolded state and the partially folded states are far from being describable as statistical coils. The current experiments show the effectiveness of long-range distance determination for investigating the structure and flexibility of partially folded conformations and the functional native state as well.

The determination of local and nonlocal interactions that direct the pathway of folding is a major objective of protein folding studies. Insights about energetically favorable interactions that are important in the folding pathway can be obtained by investigation of global structures of proteins in unfolded and partially folded states. Such structures are expected to be ensembles of multiple, interconverting conformers. In a series of related earlier studies, we were able to characterize native and nonnative structures in RNase A (McWherter et al., 1986), in peptide fragments of RNase A (Beals et al., 1991), and in BPTI[1] (Amir & Haas, 1987; Gottfried & Haas, 1992) using time-resolved dynamic nonradiative excitation energy transfer measurements (ET) between fluorescent probes covalently attached to specific

† This work was supported by the National Institute of General Medical Sciences of the National Institutes of Health (Grant GM-24893), by the U.S.−Israel Binational Science Foundation (Grant 91−170), and by equipment grants from the Basic Research Fund of the Israeli Academy of Sciences (1990) and the Russell Foundation of Miami (1991). Support was also received from the National Foundation for Cancer Research.

‡ Cornell University.

§ NIH postdoctoral fellow (1990−1993).

‖ Bar-Ilan University.

⊗ Abstract published in *Advance ACS Abstracts,* December 1, 1995.

0006-2960/95/0434-15965$09.00/0

sites along a peptide or protein chain. However, a significant limitation in the earlier studies was the poor resolution of intramolecular segmental diffusion rates because of a relatively short intrinsic donor lifetime.

In this paper, we provide a significant extension of our previous conformational studies of bovine pancreatic ribonuclease A (RNase A), a single-chain protein containing 124 amino acid residues and 4 disulfide bonds. We describe a novel and generally applicable labeling strategy which has been used here to prepare three different derivatives of RNase A, each of which is labeled with a fluorescent donor (2-naphthylalanine-amide; Nal-NH_2) at the C-terminus and an acceptor (7-carboxymethylamino-4-methyl-2*H*-1-benzopyran-2-one; CM-coum), attached specifically to the ϵ-amino group of a single lysine residue (residue 1, 61, or 104 in the three derivatives). For the current studies, we have used a donor probe with a relatively long intrinsic fluorescence decay rate in order to improve the precision in the determination of intersegmental diffusion coefficients.

Time-resolved fluorescence of both probes in the three doubly labeled derivatives was measured under solution conditions favoring either the native or unfolded conformations, both with and without intact disulfide bonds. The results were subjected to a global analysis (Haas et al., 1975, 1978a,b; Beechem & Haas, 1989; Gottfried & Haas, 1992) to yield segmental end-to-end distance (EED) distributions and well-resolved values of intramolecular diffusion coefficients of segment ends. The three derivatives selected provide details about the interactions that lead to partially and fully folded structures in the whole molecule, the C-terminal half of the molecule, and the 21-residue portion close to the C-terminus, respectively.

MATERIALS AND METHODS

Materials. The *N*-hydroxysuccinimide ester of the coumarin derivative suitable for amino group labeling (i.e., 7-carboxymethylamino-4-methyl-2*H*-1-benzopyran-2-one; common name, 7-carboxymethylamino-4-methyl coumarin) was prepared as described previously (Forster & Haas 1993); spectro-grade DMF (Fisher Scientific) was bubbled with N_2 before use to remove volatile amine contaminants; Sephadex G-25 (superfine) was from Pharmacia; Hydropore sulfopropyl-SCX ion-exchange columns were from Rainin (Woburn, MA); HPLC was carried out with a Pharmacia-LKB Bromma 2249 gradient pump module; ultra violet (uv) detection was with a Gilson 130 dual-wavelength detector (Gilson; Middletown, WI); TPCK trypsin was from Sigma (St. Louis, MO); RNase A was from Sigma and purified as described previously (Buckler et al. 1993) ; Boc-L-naphthylalanine amide was prepared as described previously (Buckler et al. 1993).

[1] Abbreviations: BPTI, bovine pancreatic trypsin inhibitor; CFIS, chain-folding initiation site; cCMP, cyclic cytidine 3′,5′-monophosphate; CM-coum, 7-carboxymethylamino-4-methyl-2*H*-1-benzopyran-2-one; coumarin-RNase, RNase A labeled at one or more of its lysine ϵ-amino groups by CM-coum; DMF, dimethylformamide; DTT, dithiothreitol; E, transfer efficiency; EED, end-to-end distance; ET, nonradiative excitation energy transfer; GdnHCl, guanidinium hydrochloride; MA-MCP, multianode microchannel plate; (*n*-124)RNase A, RNase(1-123)-Nal-NH_2 in which a lysine ϵ-amino group at residue *n* was acylated by a CM-coum probe; Nal-NH_2, 2-naphthylalanine amide; RNase A, bovine pancreatic ribonuclease A; RNase(1−123)-Nal-NH_2, RNase A derivative in which residue 124 was enzymatically replaced by a Nal-NH_2 residue; RP-HPLC, reverse-phase high performance liquid chromatography; TPCK, tosyl-L-phenylalanine-chloromethyl ketone.

Preparation of Donor-Only, Acceptor-Only, and Donor−Acceptor Labeled RNase A Derivatives. RNase(1−123)-Nal-NH_2, a derivative of ribonuclease A in which the C-terminal Val-124 was replaced by the fluorescent donor probe 2−naphthylalanine amide (Nal-NH_2), was prepared by enzymatic, C-terminal transpeptidation as described previously (Buckler et al., 1993). This donor-labeled derivative was modified at free amino groups using the *N*-hydroxysuccinimide ester of 7-carboxymethylamino-4-methyl-coumarin (Forster & Haas, 1993) as follows. RNase(1−123)-Nal-NH_2 (16 mg, 1.2 μmol) was dissolved in 2.0 mL of 0.100 M sodium phosphate, pH 7.44 at 22 °C. To this solution was added 62 μL (1.5 μmol) of a 24 mM solution of the activated coumarin in DMF (prepared immediately before use by dissolving 1.2 mg of the hydroxysuccinimide ester of the coumarin derivative in 150 μL of DMF). After 1.3 h at 22 °C, the protein fractions were separated from the low molecular weight derivatizing reagent using Sephadex G-25, with exchange into 0.1 M acetic acid. The resulting protein fraction was lyophilized and subjected to purification using sulfopropyl cation-exchange chromatography. The eluant was detected by uv absorbance simultaneously at 350 and 280 nm, and protein peaks exhibiting an integrated peak ratio for 350/280 nm of about 1.2, indicating mono-labeling (see Results), were collected.

The components of the resulting fractions were separated by RP-HPLC. Multiple peaks were seen for this second dimension of chromatography; therefore, fractions from each peak were isolated and resubjected to a second or third separation (under the same reverse-phase conditions as above) until a chromatographically homogeneous sample was obtained. The complete modification procedure described above was repeated, and the final yield of doubly labeled protein from a total of ≈40 mg of donor-only protein was ~150−200 μg of each of the Lys-1 and Lys-104 and ~1 mg of the Lys-61 doubly labeled derivatives.

The acceptor-only sample of RNase A (coumarin-RNase) was prepared by treating a solution of 2 mg (0.14 μmol) of RNase A in 0.20 mL of 0.1 mL sodium phosphate, pH 7.6 at 22 °C, with 36 μL (2.1 μmol) of a 0.059 M solution of the activated coumarin derivative (prepared immediately before use by dissolving 0.7 mg of active ester in 36 μL of DMF). The reaction mixture was vortexed periodically over 1 h, and the derivatized protein was desalted over Sephadex G-25 using an eluant of 0.1 M HOAc and lyophilized.

Tryptic Mapping and Characterization of Labeling Sites. The C-terminally modified donor-only protein sample and the doubly labeled derivatives (20−50 μg of each) were characterized by tryptic mapping as described previously (Buckler et al., 1993). Tryptic peptides for doubly labeled derivatives were analyzed by RP-HPLC as described previously (Buckler et al., 1993) and were detected simultaneously by uv absorption at 210 nm and by fluorescence (excitation: 280 nm; emission: >420 nm). Since the donor (Nal) does not fluoresce above 400 nm, fractions exhibiting fluorescence indicate the presence of acceptor chromophore. These were lyophilized for mass spectrometric and amino acid analyses. Mass spectrometry was carried out at the Cornell Biotechnology Center using a Finnegan Lasermat. External peptide standards of known composition and mass were used, and the precision was approximately 0.1%. Amino acid analyses were carried out at the Cornell

Biotechnology Center using the Waters Picotag system (Waters, Division of Millipore, Milford, MA).

Activity Assays. Activity assays of modified protein samples relative to native were carried out with an assay buffer of 20 mg/L of cCMP in 0.10 M Tris, 2 mM EDTA at pH 6.94 and 23.0 °C (Crook et al., 1960) as described previously (Buckler et al., 1993). Stock solutions of the three doubly labeled derivatives with donor at the C-terminus and acceptor at Lys residues 1, 61, and 104, respectively, were in 0.100 M KOAc, pH 3.94, 0.200 M KCl at concentrations of 4.24, 2.78, and 7.09 × 10^{-6} M, respectively (based on ϵ_{350} = 18 000 cm^{-1} M^{-1}). Triplicate measurements were made, from which mean activities and the 95% confidence uncertainty ranges were determined.

Measurement of Protein Concentrations. Protein concentrations were determined from uv absorbance at 280 nm for RNase A and RNase (1−123)-Nal-NH_2 using extinction coefficients of 9 500 cm^{-1} M^{-1} and 14 885 cm^{-1} M^{-1}, respectively (Buckler et al., 1993). Protein concentrations of acceptor-containing samples were determined at 350 nm using an extinction coefficient of 18 000 (±2 200) cm^{-1} M^{-1} at the 95% confidence level. This value for the protein-bound coumarin chromophore was used for all doubly labeled derivatives and was determined by uv absorbance measurement and quantitative amino acid analysis [as described previously for the donor-only derivative (Buckler et al., 1993)] of the doubly-labeled derivative with the acceptor at Lys-61 at 22 °C in 0.1 M HOAc.

Ultraviolet Absorbance, Steady-State Fluorescence, and Fluorescence Lifetime Measurements. Ultraviolet absorption measurements were made on a modified Cary 14 spectrophotometer (Denton et al., 1982). Corrected and noncorrected steady-state fluorescence emission spectra were obtained on a Perkin-Elmer MPF-44B fluorometer equipped with a Differential Corrected Spectral Unit (DCSU) accessory.

Fluorescence decay data were obtained by the single-photon counting method with an experimental setup described previously (Gottfried & Haas 1992). For the instrument response data, a dilute glycogen scattering solution was used in the sample compartment, and the emission monochromator was set to 295 nm; for the donor emission data, a 2 in. × 2 in. × 3-mm-thick broad-band interference filter was placed between the sample and emission monochromator, which was set to 340 nm; and, for the acceptor emission data, a 2 in. × 2 in. × 3-mm-thick KV-450 long-pass filter (Schott Glass, Co; Durya, PA) was placed between the sample and the emission monochromator, which was set to 460 nm. Emission intensity was attenuated by a filter so that the pulse detection rate was less than 0.1% of the excitation pulse rate, and the excitation was at a polarization angle of 55° relative to the excitation−emission plane using a double Fresnel rhomb to abolish polarization effects on the recovered decay data (Shinitzky, 1972).

Quantum Yield Measurements and Spectral Overlap Calculations. Förster's (1948) critical distance, R_o, was calculated from the relation:

$$R_o = [(9.79 \times 10^3)(\kappa^2 n^{-4} Q_D J)]^{1/6} \text{ Å} \quad (1)$$

The orientation factor, κ^2, relating the relative geometric orientation of the probes, was assumed to attain the limiting value of 2/3 since both probes exhibit mixed polarization, reducing uncertainties introduced by this assumption to less than 10% (Haas et al., 1978b; see also Discussion section). The refractive index, n, of the sample solution was determined using an Abbe refractometer at the sodium D line at 23 °C. The donor quantum yield, Q_D, and the spectral overlap values, J, between donor emission and acceptor absorption spectra, were calculated as described below.

The quantum yield for a model donor compound, Boc-Nal-NH_2, prepared as described previously (Buckler et al., 1993), in 50 mM NaOAc, pH 5.0, 22 °C, was determined with the steady-state spectrofluorimeter by the comparative method (Chen et al., 1969) using tryptophan (in the same buffer) as a reference [quantum yield, Q_R = 0.14 (Kirby & Steiner, 1970)]. Both Boc-Nal-NH_2 and Trp were purified by reverse-phase HPLC immediately before fluorescence measurements, and the eluant collected from the purification was used as a primary stock solution. Aliquots of these solutions were diluted with the above aqueous buffer in order to give a concentration yielding 0.200 (± 0.002) AU at 280 nm for each secondary stock solution, from which subsequent serial dilutions were made. The corrected steady-state fluorescence emission spectra for both sample and reference were measured at several concentrations (280 nm excitation, 5 nm band width, 290−500 nm emission range, measurements in triplicate), and the traces were digitized. The ratios of integrated emission of the Boc-Nal-NH_2 to Trp solution, I_S/I_R, were then used to calculate the quantum yield of Boc-Nal-NH_2 (Q_S) from eq 2. It should be noted that, for each ratio determined, the absorbance of both reference and unknown at the excitation wavelength were identical.

$$Q_S = 0.14\ (I_S/I_R) \quad (2)$$

The quantum yield for Boc-Nal-NH_2, 0.163 ± 0.032 (at 95% confidence, assuming no error in the reference value of 0.14), was calculated using eq 2 and is the average of five independent measurements at concentrations from 4.00 × 10^{-7} to 2.00 × 10^{-6} M. The fluorescence lifetime of this same stock solution of Boc-Nal-NH_2, adjusted to 0.05 AU at 280 nm in 50 mM NaOAc, pH 5.0, 22 °C, was then measured, using the time-resolved apparatus and methods described previously (Buckler et al., 1993), giving a lifetime (τ_S) of 36.8 ns for a fit to monoexponential decay (χ^2 = 1.36). This value for Boc-Nal-NH_2 and its associated quantum yield of 0.16 were then used as a reference to determine the quantum yield of donor-labeled RNase A samples (Q_D), under all conditions for which the donor fluorescence lifetime τ_D was measured, using eq 3:

$$Q_D = (\tau_D/\tau_S)(Q_S)$$

$$Q_D = (\tau_D/36.8)(0.16) \quad (3)$$

The spectral overlap value, J, was calculated from eq 4,

$$J = \frac{\int F_D(\lambda)\epsilon_A(\lambda)\lambda^4\, d\lambda}{\int F_D(\lambda)\, d\lambda}\ \text{M}^{-1}\ \text{cm}^3 \quad (4)$$

where $F_D(\lambda)$ is the corrected steady-state emission spectrum of the donor under the given set of solution conditions in units of relative intensity per unit wavelength, $\epsilon_A(\lambda)$ is the acceptor absorption spectrum in units of molar absorptivity

(M^{-1} cm^{-1}), and λ is the wavelength of emission (in centimeters).

Preparation of Native, Denaturing, and Reducing Solutions for Time-Resolved Analysis. Concentrated stock solutions (ca. 0.5 mM) of singly and doubly labeled protein samples in H_2O were prepared and stored at −30 °C. These concentrated samples were used for fluorescence lifetime measurements after dilution to 10 μM in the desired buffers defined as follows: (i) native-favoring conditions (N), in 50 mM NaOAc, pH 5.0; (ii) oxidizing-denaturing conditions (U), i.e., with intact disulfide bonds, in the presence of 6.2 M GdnHCl, pH 5.0 in 50 mM NaOAc; (iii) reducing-denaturing conditions (R), i.e., with disulfide bonds reduced by treating the protein sample (100 μM) with 6.7 M GdnHCl/140 mM DTT in 0.1 M Tris, pH 8.0 at 22 °C for 6 h, followed by dilution (1:10) of this solution to final conditions of 10 μM labeled RNase A derivative, 6.7 M GdnHCl, 14 mM DTT, pH 5.0 in 50 mM NaOAc; and (iv) reducing−renaturing conditions (R_N), by initial reduction/denaturation of the sample as described in (iii) and then dilution of the sample to final conditions of 10 μM labeled RNase A derivative, 0.60 M GdnHCl/14 mM DTT, pH 5.0 in 50 mM NaOAc.

Reversible Thermal Unfolding Transitions Curves. Reversible thermal denaturation−renaturation was demonstrated for the donor-only sample, RNase(1−123)-Nal-NH_2 following previously reported methods (McWherter et al., 1986).

Model and Data Analysis. The EED distribution parameters and diffusion coefficients were extracted from the donor and the acceptor fluorescence decay measurements by least squares curve fitting (Marquardt procedure). The calculated decay curves were obtained from numerical solutions of a modified version of a second-order differential diffusion equation as described previously (Haran et al. , 1992; Ittah & Haas, 1995):

$$\frac{\partial P(r,t)}{\partial t} = D\frac{\partial}{\partial r}\left[\exp\{-U(r)/k_BT\}\frac{\partial}{\partial r}\exp\{U(r)/k_BT\}P(r,t)\right] - k(r)P(r,t) \quad (5)$$

where $P(r,t)$ is the probability density for an excited state donor at a distance r from the acceptor at time t after excitation, D is the segmental diffusion coefficient, and $U(r)$ is a distance-dependent potential of mean force. This potential was taken to be harmonic [$U(r) = a(r - b)^2$] where a and b are the parameters that together determine the width and mean of the EED distribution. The quantity $k(r)$ is the reaction term which includes the spontaneous decay and the Förster energy transfer term, as shown in eq 6:

$$k(r) = (1/\tau_D)[1 + (R_o/r)^6] \quad (6)$$

where τ_D is the fluorescence lifetime of the donor in the absence of an acceptor and R_o is the Förster critical distance. In the case of biexponential decay of the donor fluorescence, τ_D, care was taken to account for the correct R_o for each component with the proper weighting (Haran, et al., 1992).

The fluorescence decay of the donor probe was measured for the derivative, designated donor-only (the D-experiment, a reference experiment which yields τ_D), and for the doubly labeled derivative (referred to as the DD experiment, the ET experiment). The fluorescence decay of the acceptor was also measured for two separate derivatives, for the acceptor-monolabeled derivative (the A experiment, no donor, a reference experiment for determination of τ_A) and for the doubly labeled derivative under excitation at the wavelength of donor excitation (the DA experiment, the second ET experiment).

The model described by eq 5 was then fit to the four data sets simultaneously (globally analyzed) using a modified version of the Globals software package (University of Illinois, Urbana; Beechem & Haas, 1989) compiled under the UNIX operating system. The experimental setup for obtaining fluorescence decay curves was based on a synchronously pumped dye laser which was described by Gottfried and Haas (1992). All samples were excited with 295 nm pulses followed by detection of photon emission after (i) optical filtering with a broad-band interference filter and monochromator set at 340 nm to observe donor emission in the D and DD experiments, and (ii) optical filtering with a 450-nm long-pass filter and monochromator set at 460 nm to observe acceptor emission in the A and DA experiments. Decay data were collected in 1024 channels, 0.20 ns/channel (205 ns full scale) for the D and the DD experiments, and in 512 channels, 0.20 ns/channel (102 ns full scale) for the A and the DA experiments. In all data sets, data fitting was started two channels after the sharp lamp peak to minimize convolution errors for narrow-width lamp pulses (the excitation wavelength was 295 nm in all four experiments). The goodness of the fit for acceptance of the best fit parameters was judged by three criteria: minimum χ^2, random distribution of residuals, and minimal autocorrelation of residuals. Error ranges of the parameters were determined by the rigorous analysis procedure at the 98% confidence limit (as defined by the F-statistic).

For the analysis of the decay data of samples under conditions favoring the native conformation of RNase A (N), a bimodal distribution function (sum of two Gaussian functions) for the EED was used. For all three doubly labeled derivatives under these conditions, inclusion of this second component for the EED distribution gave significant improvement in global χ^2 relative to a single distribution form. The second Gaussian component in each case was characterized by a large mean and width and accounted for (10 ± 4)% of the total area of the EED distribution. For all other conditions except N, a single component EED was used in the data analysis since no significant improvement in the goodness of fit (reduction in χ^2 by more than 15%) could be obtained by the bimodal distribution function.

RESULTS

Labeling and Purification of Protein Derivatives. RNase A with a donor probe, 2-naphthylalanineamide, at the C-terminus had been prepared and characterized previously (Buckler et al., 1993). To obtain doubly labeled samples, the donor-only material was modified by acylation with the carboxyl-activated derivative of 7-carboxymethylamino-4-methyl-coumarin, shown in its protein-bound form in Figure 1. The ten Lys ϵ-amino groups and the single α-amino group were the potential labeling sites in this reaction. Two sequential types of chromatography were used to separate the heterogeneous population of doubly labeled products (Figure 2). A first separation by cation exchange chroma-

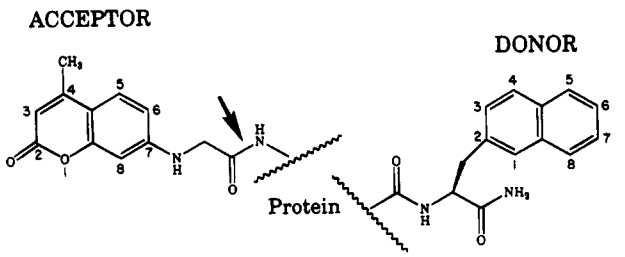

FIGURE 1: Chemical structures of the acceptor probe, 7-carboxymethylamino-4-methyl-coumarin (left) and the donor probe, 2-methylnaphthyl side chain of 2-L-naphthylalanine amide (right) after conjugation to protein. The arrow indicates the amide bond formed between the activated coumarin reagent and protein amino group.

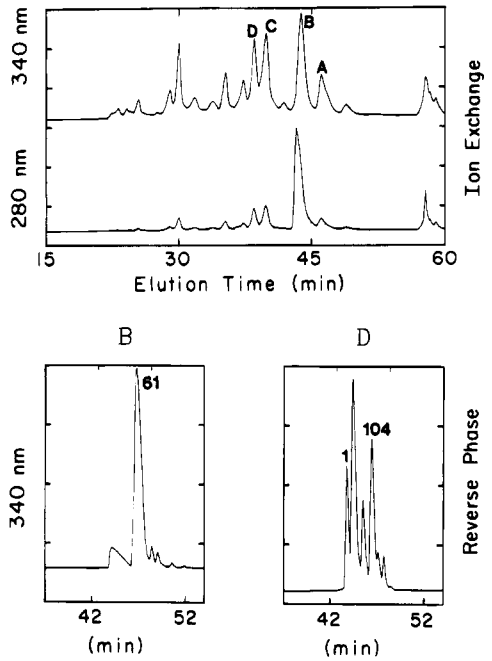

FIGURE 2: Cation-exchange separation of the products from the acylation of RNase(1−123)-Nal-NH_2 with the *N*-hydroxysuccinimide ester of 7-carboxymethylamino-4-methyl-courmarin, i.e., mixture of (*n*-124)RNase A derivatives (top), and second dimensions of reverse-phase HPLC (bottom) of the indicated fractions from ion exchange. High performance cation exchange chromatography was carried out with a 2.5 cm × 10 cm SCX-Hydropore sulfopropyl cation exchange column using a gradient of 0 to 0.15 M NaCl over 47 min in 20 mM Hepes, 1 mM EDTA, pH 7.8 at 9 mL/min. Reverse-phase HPLC was carried out with a 1.0 × 27 cm Dynamax C-18 HPLC column with a linear gradient of 20% to 40% MeCN in 0.09% aqueous TFA over 40 min at 3 mL/min. The numbers in the lower traces correspond to the lysine sites of modification as identified by tryptic mapping (see Figures 3−5; Tables 1 and 2).

tography provided the first dimension. By monitoring the ratio of uv absorption at 350 nm to 280 nm, the degree of labeling was estimated for each fraction. Those fractions with a 350 nm/280 nm uv absorption ratio of ca. 1.2 consisted predominantly of the desired samples (with a single acceptor and single donor per protein). It was found that a molar ratio of ca. 1.5:1 of acceptor acylating reagent over donor-labeled protein provided optimal yields of the desired singly-acceptor-labeled species.

The fractions of interest from the ion-exchange purification exhibiting the desired absorbency ratio were collected and subjected to a second purification dimension by RP-HPLC (Figure 2). Fraction B from the ion-exchange dimension, when subsequently separated by RP-HPLC, consisted predominantly of starting donor-only material together with a species doubly-labeled with both the donor and a single-site acceptor. The position of the acceptor label for this derivative was determined to be Lys-61 (see below). Fraction D from ion-exchange, which eluted at a different position and was therefore free of donor-only sample, proved to be heterogeneous and was resolved further by the second dimension of RP-HPLC (Figure 2). Two peaks of interest were isolated and determined to arise from the derivatives with acceptor label at Lys-1 and Lys-104 (see below). In each case, sequential purification steps of isolated fractions in the reverse-phase dimension were carried out until a chromatographically homogeneous sample was obtained. The purified materials were determined to be chemically homogeneous, with a single donor probe at the C-terminus and acceptor probes at Lys-1, −61, or −104, as described in the next section.

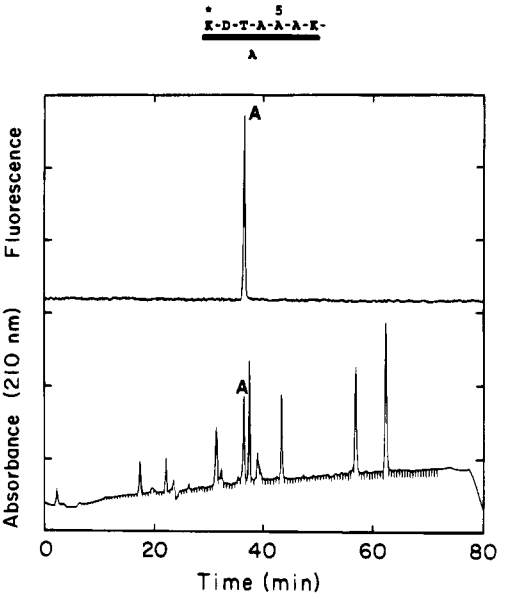

FIGURE 3: RP-HPLC of the tryptic map of the reduced and S-carboxymethylated derivative with the acceptor at Lys-1 and the donor at the C-terminus. Separation was carried out with a Waters 0.8 × 10-cm Nova-Pak/Radial-Pak C-18 column using a linear gradient of 2% to 40% MeCN in 0.09% aqueous TFA over 68 min at 1 mL/min. The schematic above the chromatogram shows the amino acid sequence and site of labeling at a specific Lys residue (*) within the peptide fragment, labeled "A." The upper trace in the chromatogram shows coumarin fluorescence (excitation = 280 nm, emission > 420 nm) and, therefore, identifies any peptide(s) containing the acceptor label; the lower trace is uv absorbance. The single coumarin-labeled tryptic fragment (showing fluorescence in the trace) was identified by amino acid and mass spectral analysis (Tables 1 and 2).

Characterization of Acceptor Labeling Site. Tryptic maps of reduced and carboxymethylated derivatives were used to identify acceptor labeling sites. All tryptic fragments containing label could be determined directly by fluorescence detection, as shown in Figures 3−5. Materials from peaks exhibiting characteristic coumarin fluorescence were collected and identified by matrix-assisted laser-desorption ionization mass spectrometry (Table 1) and amino acid analysis for the larger peaks (Table 2). It was observed that acylation of the ϵ-amino groups of lysine by the acceptor prevented tryptic cleavage at this site. The masses and amino acid compositions found for the fluorescent peaks were consistent, in each sample examined here, with a single labeling site for each of the three derivatives. For the

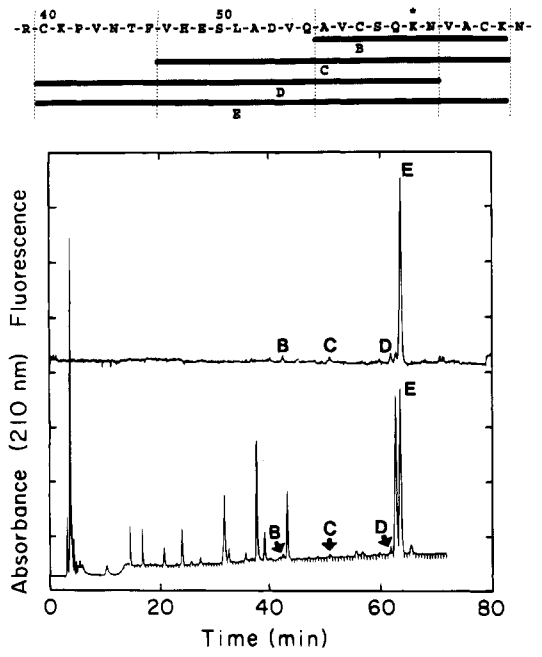

FIGURE 4: RP-HPLC of the tryptic map of the reduced and S-carboxymethylated derivative with the acceptor at Lys-61 and the donor at the C-terminus. Separation, detection, and characterization of peptides were carried out as in Figure 3. The schematic above the chromatogram is as described for Figure 3, showing site of labeling (*) and tryptic fragments B–E.

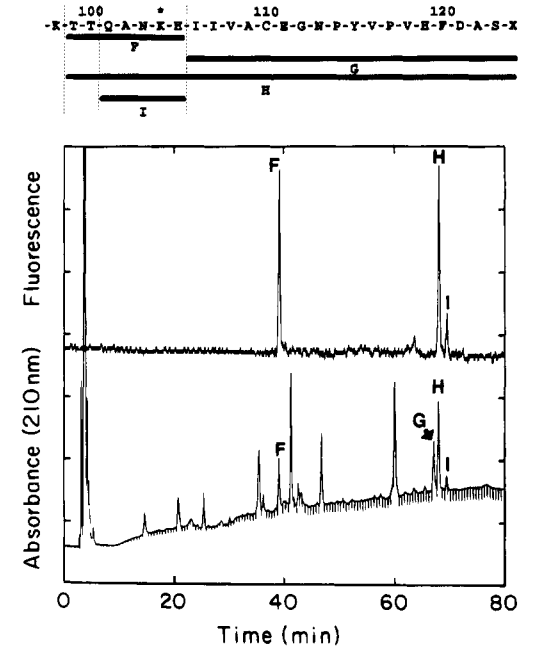

FIGURE 5: RP-HPLC of the tryptic map of the reduced and S-carboxymethylated derivative with the acceptor at Lys-104 and the donor at the C-terminus. Separation, detection, and characterization of peptides were carried out as in Figure 3. The schematic above the chromatogram is as described for Figure 3, showing site of labeling (*) and tryptic fragments F–I. ($X \equiv Nal - NH_2$). Peak G is not labeled by acceptor, but was isolated and identified (see Table 1) to confirm nonspecific cleavage after His 105.

derivative identified in Figure 3, the possibility of labeling at the α-amino group of Lys-1, instead of at its ϵ-amino group, could not be unequivocally ruled out based on the available data. However, a free ϵ-amino group at Lys-1 should produce an alternate tryptic cleavage site after this residue, which was not observed (Figure 3, Tables 1 and 2).

Table 1: Mass Spectral Analysis of Acceptor-Labeled Tryptic Peptides from Derivatives (1–124)RNase A, (61–124)RNase A, and (104–124)RNase A

peak[a]	amino acid sequence[b]	calculated (M + H)[c]	found (m/z)[d]
A(1)	1–7	934	934
B(61)	56–66	1482	1484
C(61)	47–66	2460	2463
D(61)	40–62	2848	2851
E(61)	40–66	3307.5	3307
F(104)	99–105	1014.5	1013
G(104)[e]	106–124	2185	2186
H(104)	99–124	3180.5	3180
I(104)	101–105	812.5	818

[a] Peptide isolated from peptide maps as indicated in Figures 3–5. The number in parentheses indicates the position of the acceptor label. [b] Proposed amino acid sequence based on mass spectral and amino acid (Table 2) analyses. [c] Protonated mass (average for naturally occurring isotopes) calculated for amino acid sequence indicated in column 2. [d] Mass to charge ratio (m/z) for tryptic peptide as determined on a Finnegan Lasermat matrix assisted laser desorption ionization time of flight mass spectrometer. [e] Nonlabeled fragment identified to confirm nonspecific cleavage site at His-105.

Table 2: Amino Acid Analysis[a] of Acceptor-Labeled Tryptic Peptides from Derivatives (1–124)RNase A, (61–124)RNase A, and (104–124)RNase A

amino acid	fragment A (1–7)	fragment E (40–66)	fragment F (99–105)
Asx	–	3.0 (3)	1.1 (1)
Glx	1.3 (1)	3.1 (3)	1.2 (1)
Ser	0.76 (0)	2.0 (2)	0.87 (0)
Gly	1.1 (1)	0.48 (0)	1.1 (0)
Arg	0.34 (0)	–	0.36 (0)
His	–	0.80 (1)	0.76 (1)
Thr	0.94 (1)	1.1 (1)	1.8 (2)
Ala	2.6 (3)	3.0 (3)	1.2 (1)
Pro	–	1.1 (1)	–
Val	–	4.6 (5)	–
CM-Cys	–	2.8 (3)	–
Leu	0.35 (0)	1.1 (1)	0.43 (0)
Phe	–	1.1 (1)	–
Lys	1.7 (2)	2.7 (3)	0.75 (1)

[a] Amino acid analysis was carried out with a Waters Picotag system on hydrolyzates of tryptic peptides indicated in Figures 3–5. Proposed amino acid sequences are indicated in parentheses above each column (for a complete sequence of RNase A, see Richards & Wyckoff, 1971). Recoveries <0.3 residues are indicated by "–."

This strongly suggests that the labeling site was indeed at the ϵ-amino group of Lys-1 rather than at its α-amino group. Furthermore, for the purposes of this study, labeling at either (or both) α- or ϵ-amino positions of Lys-1 should result in small overall distance differences relative to the donor probe at residue 124, especially for partially denatured states. Nonspecific cleavage sites (i.e., at positions other than after Arg or Lys) were observed in the tryptic maps for both the Lys-61 and Lys-104 derivatives; however, all resulting fragments were consistent with a single labeling site. In particular, minor cleavages after Phe 46, Gln 55, and Asn 62 (Figure 4) and after Thr 100 and His 105 (Figure 5) were observed for the Lys-61 and Lys-104 derivatives, respectively.

Reversible Thermal Unfolding/Folding Transitions of Donor-Only and Enzymatic Activity of Labeled RNase A. In order to assess the suitability of the labeled derivatives for folding studies, a reversible, thermal unfolding transition was measured for the donor-only species. This was particularly critical for the C-terminally modified derivative since this

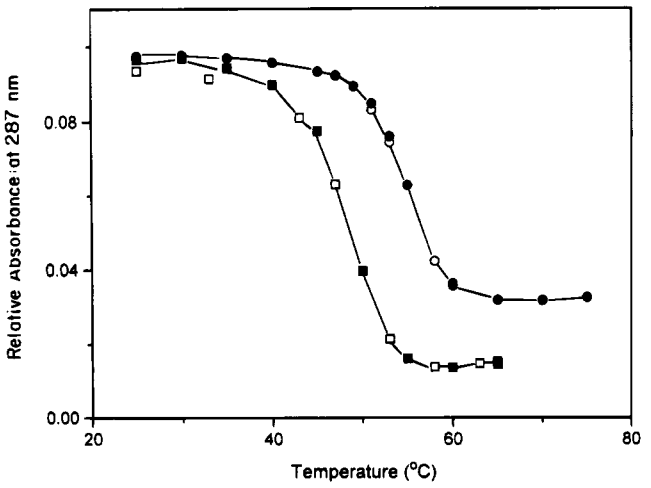

FIGURE 6: Reversible thermal unfolding/folding transition in 0.10 M NaOAc, 0.2 M KCl, pH 3.95 for RNase A at 32 μM (circles) and RNase(1−123)-Nal-NH_2 (squares) at ~20 μM. The filled symbols show heating, and open symbols show cooling of the sample. T_m for RNase A = 54.4 °C; T_m for RNase(1−123)-Nal-NH_2 = 48.3 °C.

region of the molecule is known to be buried in the native conformation and also plays a critical role in directing the folding, as assessed by enzymatic truncation studies (Fujioka & Scheraga, 1965; Burgess & Scheraga, 1975; Chavez & Scheraga, 1980a). The observed thermal transition for RNase(1−123)-Nal-NH_2 was fully reversible and exhibited a depression in melting temperature of 6.1 °C, relative to the native protein, as shown in Figure 6. Reversible thermal transitions were not determined for the doubly labeled derivatives because of limited quantities of the samples; however, such modifications were designed to minimize structural perturbation of the folded conformation since they were targeted to surface-exposed groups of the molecule under conditions favoring the native state. It has previously been shown that extensive modification at Lys ϵ-amino groups, e.g., with poly(D,L-alanine), produces derivatives that retain full activity (Cooke et al., 1963).

Enzymatic activity relative to native RNase A was measured for each derivative, giving values of 87 ± 5%, 94 ± 7%, 79 ± 10%, and 207 ± 15% for RNase(1−123)-Nal-NH_2, (104−124)RNase A, (61−124) Rnase A, and (1−124) RNase A, respectively. The (61−124)RNase A and (104−124)RNase A derivatives and the donor-only RNase(1−123)-Nal-NH_2 each exhibited activity approximately 90% that of native RNase A. Interestingly, the derivative modified at Lys-1, (1−124)RNase A, exhibited an activity roughly 2-fold higher than that of the native protein, suggeting that the native conformation and chemical composition of RNase A is not optimized for maximal rate of catalytic hydrolysis of this low-molecular-weight substrate. The origin of this enhanced activity was not investigated further.

Spectral Overlap Calculations. The probes were chosen to provide effective spectral overlap of donor emission with acceptor absorption, as shown in Figure 7. Irradiation of the sample at 295 nm in the time-resolved fluorescence measurements allowed effective donor excitation while minimizing excitation of intrinsic Tyr residues (λ_{max} = 278 nm). Förster's critical distance was obtained for each solution condition studied (Table 3), using values of Q_D, n, and J obtained as described in the Materials and Methods section. For this pair of donor−acceptor probes in the range

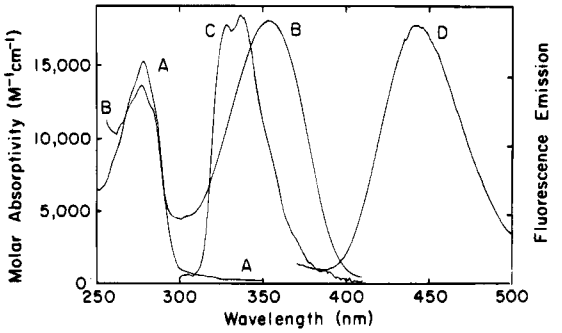

FIGURE 7: Ultraviolet absorption spectra, and corrected steady-state fluorescence emission intensity spectra (in arbitrary units) of the chromophores attached to the protein. Molar absorptivity profile of RNase(1−123)-Nal-NH_2 (A) and of coumarin-labeled RNase A (B); corrected fluorescence emission spectrum of RNase(1−123)-Nal-NH_2 with excitation at 290 nm, excitation slit width = 3 nm (C) and of coumarin-labeled RNase A with excitation at 350 nm, excitation slit width = 3 nm (D). Measurements shown here for RNase(1−123)-Nal-NH_2 were in 0.1 M HOAc at 22 °C and for coumarin-labeled RNase A were in 50 mM NaOAc, pH 5.0 at 22 °C. The spectral overlap between donor emission (C) and acceptor absorption (B) fulfills the fundamental requirement for nonradiative excitation energy transfer to occur.

of solution conditions studied, the overlap integrals, J, are close to 1.8 × 10^{-14} M^{-1} cm^3 in all cases, and R_o's range from 25 to 29 Å. For the intrinsic donor lifetime (τ_D), measured using the donor-only sample, it was observed that (i) addition of denaturant caused significant shortening of the lifetime (from 44 ns in N to 26 ns in U), and (ii) the presence of DTT resulted in a small second component (Table 3; see further discussion in the following section).

The transfer efficiency, E, was calculated from the reduction of the intrinsic donor fluorescence lifetime (τ_D) in the doubly labeled samples (τ_{DA}), $E = 1 - \tau_{DA}/\tau_D$. As expected, τ_{DA} was shorter than τ_D and not monoexponential (Table 3). These results reflect multiple transfer rates which were analyzed in terms of distributions of interprobe distances and segmental motions during the lifetime of the donor excited state.

Decay Curves. Time-resolved fluorescence data were fit to the model shown in eq 5 as described elsewhere (Haran et al., 1992), and an example of the plots of the fits of the model after global analysis to all four data sets for the (104−124)RNase A derivative in the R state is shown in Figure 8. The means and widths of the EED distributions as well as the diffusion coefficients D, obtained under all conditions, are shown in Table 4, and the distributions are shown in Figure 9. The donor-only reference experiment demonstrated small deviations from a monoexponential fit when DTT was present (the R and R_N states, Table 3). A second short-lived component contributed less than 3% to total photon emission (see further discussion in the Control Experiments section).

DISCUSSION

The main objective of the present study was to search for conformations that arise from specific local and nonlocal interactions in the unfolded, and partially and fully folded, states of RNase A. Folding is thought to arise initially from a few effective interactions in chain-folding initiation sites (CFIS) that direct further folding steps (Matheson & Scheraga, 1978; Wright et al., 1988; Montelione & Scheraga, 1989).

Table 3: Parameters for Calculation of Förster's Critical Distance (R_o), and Results of the Time-Resolved Measurements

conditions	position labeled[a]	$\tau_i(\alpha_i)$[b] (ns)	$\langle\tau\rangle$[c]	χ^2	n[d]	J × 10^{14} (M^{-1} cm^3)	Q_D	R_o (Å)	E[e]
native (N state)	D	43.91(2.98)	43.91	1.44	1.332	1.8	0.19	29.4	–
pH 5.0, 22 °C, 0.05 M NaOAc	A	4.88 (2.38)	4.88	1.21					–
	104	41.77(1.10), 11.92(1.02), 1.04(3.39)	11.19	1.74					0.75
	61	39.67(0.381), 10.33(0.267), 0.929(1.06)	11.04	1.47					0.75
	1	40.80(0.349), 11.50(1.96), 3.58(1.11)	11.92	1.33					0.73
disulfide-intact denatured (U state)	D	25.68(2.11)	25.68	1.32	1.443	1.7	0.11	25.3	–
6.20 M GdnHCl	A	4.09(3.38)	4.09	1.36					–
pH 5.0, 22 ° C, 0.05 M NaOAc	104	19.89(1.51), 4.34(0.572)	15.62	1.45					0.39
	61	19.91(0.897), 5.83(0.432)	15.33	1.49					0.40
	1	25.7(1.59), 1.71(0.196)	23.07	1.56					0.10
reduced-denatured (R state)	D	24.12(2.22), 2.43(0.275)	21.73	1.53	1.443	1.8	0.10	24.6	–
6.71 M GdnHCl, 14 mM DTT,	A	3.95(6.69)	3.95	1.24					–
pH 5.0, 22 °C, 0.05 M NaOAc	104	18.20(2.17), 3.48(1.13)	13.16	1.47					0.39
	61	23.11(2.19), 5.03(0.14)	22.02	1.94					ND
	1	23.58(1.75), 3.52(0.18)	21.71	1.42					ND
Reduced-native like (R_N state)	D	27.81(1.4), 4.23(0.267)	24.03	1.66	1.345	1.9	0.12	26.7	
0.60 M GdnHCl, 14 mM DTT,	A	4.29(4.71)	4.29	1.77					
pH 5.0, 22 °C, 0.05 M NaOAc	104	20.18(0.75), 10.32(0.892), 1.84(0.797)	10.58	1.92					0.56
	61	50.18(0.029), 22.89(1.02), 3.4(0.426)	17.80	1.27					0.26
	1	27.26(1.72), 8.00(0.356)	23.96	1.88					ND

[a] Donor-only RNase A (D), acceptor-only RNase A (A), or lysine position modified for the doubly labeled derivative. [b] Recovered lifetimes (τ_i) and preexponential factors(α_i, not normalized) of exponential fits to time resolved fluorescence data for donor-only (D), acceptor-only (A), or doubly labeled proteins. Single through triple exponential fits were carried out for doubly-labeled samples. A triple exponential fit was chosen as a best fit only if it resulted in a reduction in χ^2 of at least 15% relative to the double exponential fit. [c] Lifetime averages ($\Sigma\alpha_i\tau_i/\Sigma\alpha_i$) for multiexponential fits. [d] Refractive index at the sodium D line. [e] Transfer efficiency determined from the relation: $E = 1 - \tau_{DA}/\tau_D$, where τ_D and τ_{DA} are the lifetimes of donor-only and doubly-labeled proteins, respectively. Lifetime averages ($\Sigma\alpha_i\tau_i/\Sigma\alpha_i$) from the parameters in this table were used to calculate τ_D and τ_{DA} for decays that were not monoexponential. ND, not detectable, transfer efficiency ≤0.01.

Table 4: Recovered Distance Distribution and Diffusion Parameters from Global Analysis of Time-Resolved Fluorescence Decay Data

conditions[a]	acceptor position[b]	mean distance (Å)[c]	σ (Å)[d]	diff. coeff. ($Å^2$/ns)[e]	(χ^2)[f]
native (N state)	104	9.8 (9.3−11.2)[g]	4.1 (3.8−4.6)	0(0−0.3)	2.45
pH 5.0, 22 °C	61	12.0 (9.7−13)[g]	4.5 (3.0−5.7)	0(0−2.1)	1.81
	1	22.0 (21.3−23.4)[g]	9.2 (7.6−9.9)	5.0 (4.0−12)	1.65
disulfide-intact	104	32.0 (29.5−35.5)	12.5 (9.4−15.5)	2.9 (1.0−5.0)	1.49
denatured (U state)	61	28.8 (27.9−29.8)	12.2 (10.9−12.6)	1.5 (0.8−2.0)	2.35
	1	>50	ND[h]	ND[h]	ND[h]
reduced-denatured (R state)	104	33.3(30−37)[i]	14.0(9.5−16)[i]	4.7 (1.5−8)[i]	1.40[i]
	61	>50	ND[h]	ND[h]	ND[h]
	1	>50	ND[h]	ND[h]	ND[h]
reduced-native (R_N state)	104	22(22−25)[j]	9(9−10.6)[j]	0.5(0.17−0.52)[j]	2.09[j]
	61	38(37.7−38.3)[k]	16.2(15.55−16.2)[k]	0(0−0.5)[k]	1.87[k]
	1	>50	ND[h]	ND[h]	ND[h]

[a] Solution conditions as defined in Table 3. [b] Acceptor labeling site for doubly-labeled derivative. All derivatives have a naphthyl alanine donor as the C-terminal residue 124. [c] Mean of Gaussian distribution. [d] Standard deviation of distribution. Full width at half maximum = 2.35 σ. [e] Diffusion coefficient. [f] Global χ^2 from global analysis of four data sets. [g] For the native conditions only, fitting to a bimodal distribution significantly improved χ^2. A first component, listed in the table, corresponds to the folded state and contributed ca. 90% of the total area of the bimodal distribution for all three derivatives. A second component in each case was broad and contributed (10 ± 4)% of the total area. For the 104, 61, and 1 derivatives, the means (Å) and standard deviations (Å) of this second distribution were, respectively: (34, 16), (42, 12), and (93, 20). [h] ND = cannot be determined with satisfactory statistical significance. [i] Double-exponential decay for the donor-only experiment was used in the global analysis; recovered parameters using single-exponential decay for donor only: mean = 27.8(26.5−29.7), σ = 11.5(9.3−12.0), diff. coeff. = 1.8(0.6−3.0), χ^2 = 1.98. [j] Double-exponential decay for the donor-only experiment was used in the global analysis; recovered parameters using single-exponential decay for donor only: mean = 22.5(21.7−23.5), σ = 9.3(8.4−9.8), diff. coeff. = 0.7(0.3−1.3), χ^2 = 2.60. [k] Double -exponential decay for the donor-only experiment was used in the global analysis; recovered parameters using single-exponential decay for donor only: mean = 47.5(42−54), σ = 20.0(16.5−23), diff. coeff. = 0(0−0.5), χ^2 = 4.32.

The three derivatives studied here represent three levels of chain length, starting from the C-terminus. The C-terminal 21-residue segment (104−124) contains an antiparallel β-sheet in the native state (Wlodawer et al., 1988), the 64-residue segment (61−124) is one-half of the length of the chain, and the third derivative [(1−124)RNase A] monitors global changes and interactions between the chain ends. A major advance made in the present study is the determination of statistically significant values of the segmental diffusion parameters, D. This was achieved by the use of a pair of probes with a large τ_D/τ_A ratio.

Experimental Conditions. Control Experiments and Assumptions in the Analysis. Essential components in the global analysis of time-resolved fluorescence data are the D and A experiments which provide internal scaling with respect to the energy transfer measurements used in the global analysis. The parameters τ_D and τ_A are measured independently for each experiment, at the same time and under the same conditions (solvent composition, concentrations, time calibration, polarization, etc.) as are τ_{DA} (experiments DD and DA) for the doubly labeled samples. These parameters, which also pertain to the DD and DA experi-

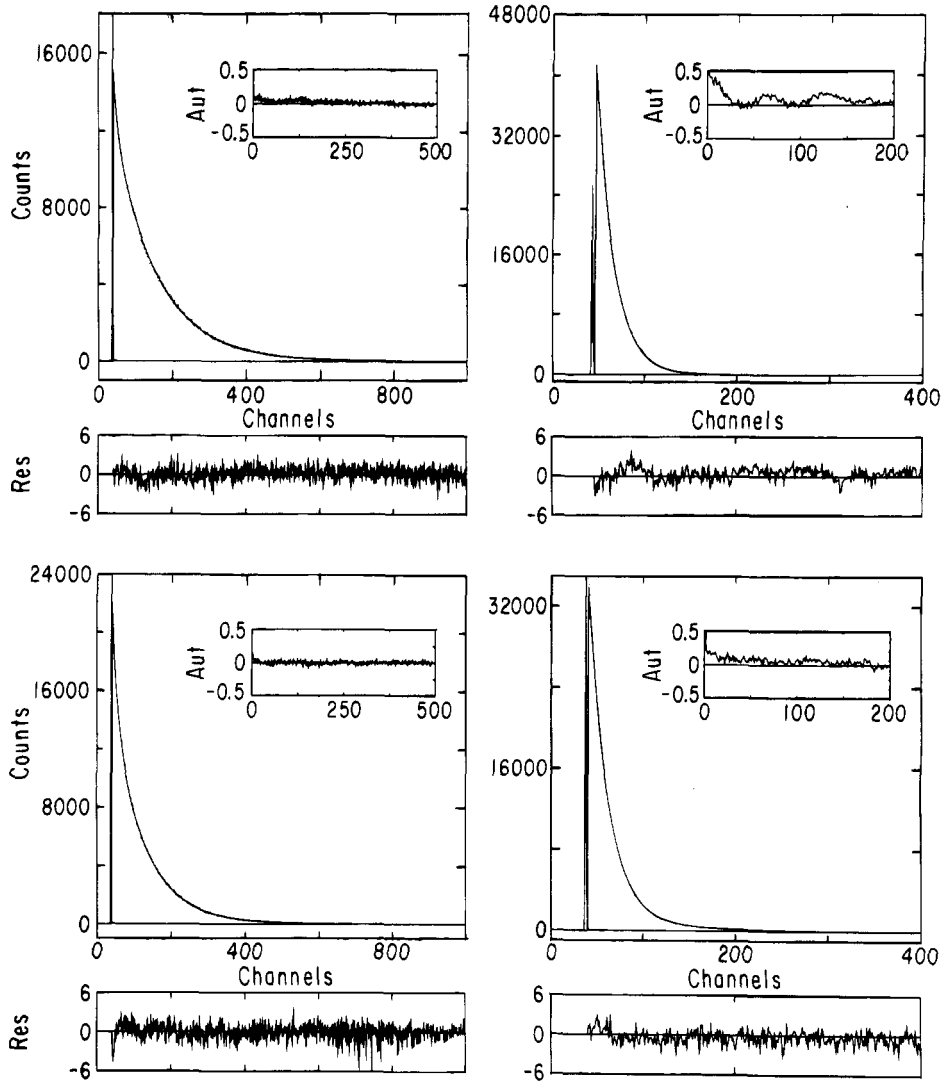

FIGURE 8: Time-resolved fluorescence curves for (104−124)RNase A and the reference derivatives in the R state (0.050 M NaOAc, pH 5.0, 6.7 M GdnHCl, 14 mM DTT after treatment with 6.7 M GdnHCl, 140 mM DTT, pH 8.0 for 6 h). Excitation at 295 nm as described in the Methods section. (•••) Experimental curves, (—) best fit theoretical curves obtained by the global analysis. A double-exponential decay was assumed for the donor-only sample. The residuals of the fits are shown in the lower blocks (Res), and the autocorrelations of the residuals (Aut) are presented for each curve in the upper right inset. The four experiments used for the global analysis are shown clockwise from upper left, with local χ^2 as indicated: fluorescence decay of the donor in the absence of an acceptor (the D experiment; the reference experiment, $\chi^2 = 2.10$), fluorescence decay of the acceptor in the absence of a donor (the A experiment; the reference experiment, $\chi^2 = 1.38$), fluorescence decay of the acceptor attached to residue 104 (the DA experiment; the ET experiment, $\chi^2 = 2.09$), and fluorescence decay of the donor in the same derivative (the DD experiment; the ET experiment, $X^2 = 2.03$).

ments, are thus not determined in a separate analysis but are introduced in the data for the global analysis. Since the main effect that is measured is the contribution of the energy transfer to the rates of fluorescence decay of the probes, the effect of many possible external interferences is thus taken into account automatically. In addition to providing internal scaling, the fluorescence lifetime data for the monolabeled derivatives also show the reproducibility of the measurements obtained in each analysis for each experimental solution condition.

For measurement of the reference, τ_A, an acceptor-only labeled derivative of RNAse A (coumarin-RNase) was prepared which was excited by the same wavelength and method as the doubly labeled samples. In principle, the doubly labeled derivative could be used for determinaation of τ_A, with excitation above the absorption band of the naphthylalanyl chromophore. The advantage of this is that it eliminates uncertainties arising from possible differences in τ_A during direct excitation in the doubly labeled protein derivatives. However, we preferred not to change the tuning of the laser system for each set of experiments (tuning the laser above 330 nm requires changing the dye in the dye laser), in order to maintain, as precisely as possible, the same instrumental conditions and calibration as for the doubly labeled derivatives. The coumarin-labeled RNase A (no donor) gave monoexponential decay under all conditions (Table 3) despite the site heterogeneity. This shows that the acceptor decay is independent of labeling site, and therefore, this sample provides a proper reference.

The presence of DTT caused the donor fluorescence decay in the absence of an acceptor (the D experiment) to deviate slightly from a pure monoexponential decay (Table 3). Second, shorter-lived components for the donor-only derivative were found in the R and R_N states with lifetimes of 2.43 ns and 4.23 ns, respectively (Table 3). These second components contribute only 1% and 3%, respectively, of the

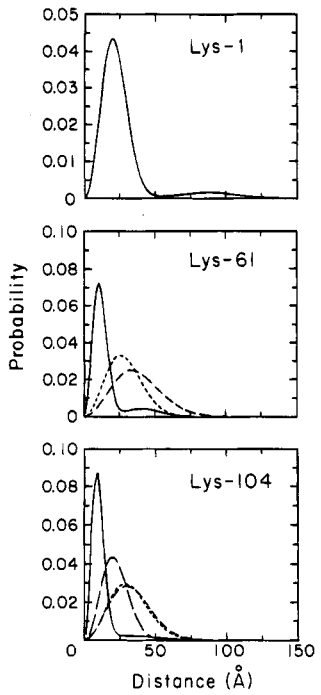

FIGURE 9: The EED distribution between the C-terminal residue (124) of RNase A and three of its lysine residues under all four solution conditions: N (native) (—), U (denatured, disulfide bonds intact) (- - -), R (denatured, disulfide bonds reduced) (— —) and R_N (folding conditions but disulfide bonds reduced) (— —). In Lys-104, the U and R curves are essentially superposed.

total photons emitted during the donor fluorescence decay in the R and R_N states (the proportion of emitted photons of component i to all emitted photons is $\alpha_i\tau_i/\Sigma\ \alpha_i\tau_i$). These experiments were analyzed on the basis of eq 5 using biexponential decay of the donor fluorescence in the absence of an acceptor (the D experiment), with the relative weights of the two components being based on the preexponential factors (results shown in Table 4). The experiments carried out in the R and R_N states were also analyzed by using the approximation that the donors obeyed single exponential decays (see legend in Table 4). The differences in the results between these two analyses were, in most cases, within the ranges of the statistical uncertainties defined by the rigorous analyses for the widths and means of the EED distributions as well as for the diffusion coefficients. The parameters obtained in the approximate (monoexponential) analysis were not very far from those shown in Table 4 because of the small contribution of the short-lifetime component to the total emission of the donor.

R_o was calculated by using experimentally determined refractive indices, donor quantum yields, acceptor absorption, and donor emission spectra. Thus, changes in transfer efficiencies due to molecular and spectroscopic effects of solvents and temperatures were also taken into account by their effect on R_o.

A frequently cited potential source of uncertainty in the magnitude of R_o is the dependence of transfer probabilities on the orientations of the probes, and an assumption is used here that the orientation factor, κ^2, attains a limiting value of 2/3. This has been discussed repeatedly in earlier publications (Jones, 1970; Hillel & Wu, 1976; Haas et al., 1978b; Stryer, 1978; Dale et al., 1979; McWherter et al., 1986; Amir & Haas, 1987; Wu & Brand, 1992; Amir et al., 1992) which showed that the error is less than 10% for probes with low anisotropy, as is the case in the present study.

A control for the absence of intermolecular energy transfer in the experimental setup (depending on the concentrations, solubilities of the derivatives, temperatures, and solvents) was made by measuring the donor fluorescence decay of a mixture of RNase(1−123)-Nal-NH_2 (donor-only) and coumarin-RNase (acceptor only) at a ratio of 1:2, respectively. The concentrations of the RNase A derivatives that were used in the time-resolved measurements were adjusted to 10 μM, and the donor fluorescence lifetimes in the presence or absence of excess coumarin-RNase agreed to within 5% for all solution conditions studied here (data not shown). This control experiment proves the absence of intermolecular energy transfer that might arise from aggregation since, at the concentrations studied (ca. 10 mM), the average distances in solution allow only negligible intermolecular transfer in the absence of aggregation.

To test for the stability of the labeled protein derivatives and of the fluorescent probes under the experimental conditions, the effect of laser-excitation irradiation on the (1−124)RNase A and (61−124)RNase A samples was assessed by several criteria before and after exposure to the laser. The fluorescence excitation and emission spectra and analytical RP-HPLC chromatograms of these derivatives, measured before and after irradiation by the laser, under conditions of the ET experiment, were identical (data not shown). As a separate control, the enzymatic activity of RNase(1−123)-Nal-NH_2 (donor-only derivative) was also measured, and showed no change before and after irradiation by the laser. These control experiments demonstrate that the conditions of the fluorescence measurements did not lead to detectable degradation of the labeled protein or of the covalently bound labels.

The Native States

The following main features of the native states of derivatized RNase A are deduced from the parameters presented in Table 4 and from the EED distributions shown in Figure 9, and are discussed in this section: (i) narrow distributions for the 21- and 64-residue segments, with recovered mean distances consistent with those expected according to the crystal structure; (ii) low diffusion coefficients (on the nanosecond timescale) for the ends of these 21- and 64-residue segments; (iii) on the contrary, the EED distribution of the full chain length [(1−124)RNase A] is broader, the mean of the distribution is smaller than expected from the crystal structure; (iv) the dynamic flexibility of the ends of the full-chain segment is high, with a diffusion coefficient even larger than that observed for the other two derivatives in the unfolded states; and (v) a second minor fraction with (10 ± 4)% of the molecules with large mean EED was found for each one of the derivatives in the native conditions. While (i) and (ii) are expected, the question is whether (iii), (iv) and (v) are not artifacts of the present experimental system rather than true properties of the native (unlabeled) RNase A.

Interprobe distances obtained by the methods described here for derivatives in the native state can be compared directly to interresidue distances obtained for the native molecule in the crystal by X-ray diffraction or in solution by ^{1}H-NMR; however, allowances must be made for finite

distances introduced by the fluorescent probes and their spacer arms. This uncertainty cannot be greater than the combined lengths of the fully extended probes from their attachment points (β-carbon of residue 124 and the ϵ-amino groups of the modified lysine residues). For the 2-naphthylalanine amide/coumarin pair used here, the probe-plus-spacer arm length is approximately 11 Å (calculated with standard bond lengths and bond angles, and dihedral angles of 180° for the spacer arms and probes shown in Figure 1, with the excitation dipole assumed to be at the center of the naphthyl or coumarin framework). The relevant position is the average position of the probe, which is shorter than the fully extended chain; therefore, the estimated value of 11 Å is only an upper limit.

The distances determined for RNase A in the crystal (Wlodawer et al., 1988) between the Val-124 β-carbon and Lys ϵ-amino groups 1, 61, and 104 are 30.8, 10.7, and 6.6 Å, respectively. Curve fitting for derivatives in the native state resulted in a large reduction in global χ^2 when a bimodal distribution function was used to describe interprobe distances. For all three derivatives, this best-fit bimodal distribution consisted of a short interprobe distance distribution component, contributing 90% of the total population, combined with a subpopulation characterized by a larger mean distance, contributing (10 ± 4) % of the total area of the bimodal distribution (Table 4, footnote *g*, and Figure 9; see below). In all three cases the minor subpopulations had broad distributions with means corresponding to the unfolded state of the segment, as found after denaturation. The major subpopulations (90%) in the three derivatives showed an average interprobe separation of 22, 12, and 9.8 Å for the (1−124), (61−124), and (104−124) segments, respectively (Table 4 and Figure 9). The latter two values are in reasonable agreement with the distances deduced from X-ray data (Wlodawer et al., 1988) which, as expected, are less than the maximal possible contribution from the spacer arms of the probes (11Å), because of averaging of the conformations of the spacer arms. However, the derived distribution mean of 22 Å for the distance between the N- and C-termini of (1−124)RNase A is *shorter* (by 9 Å) than the corresponding distance from the crystal structure. This difference may be larger than the contribution of the spacer arm of the probe. The standard deviation of the distribution for (1−124)RNase A, σ = 9.2 Å, is significantly *greater* than those obtained for (61−124)RNase A and (104−124)RNase A (Table 4), suggesting that the (1−124) distribution is not characteristic of reporter groups attached to a well-ordered, folded chain segment. The segmental diffusion coefficient was very small for the (61−124) and (104−124) segments (0 Å^2/ns), but relatively high (5 Å^2/ns) for the (1−124) segment (Table 4), close to that found for unfolded polypeptides. It is possible that, in solution, the conformation of the N-terminal segment of RNase A (at least for the labeled derivative) is significantly different from its conformation in the crystal. It has multiple conformations, and a high level of fast fluctuations on the nanosecond time scale. Is this a characteristic of RNase A, or just a result of the specific chemical modification? The retention of enzymatic activity suggests that gross changes in the native conformation did not result from chemical labeling; however, the surprisingly enhanced activity of (1−124)RNase A (ca. 2-fold greater than wild-type) could indicate small deviations of structure near the active site. Further measurements of additional derivatives of (1−124)RNase A are needed to resolve this question.

Available NMR solution-structural data for RNase A is also consistent with a dynamic conformational ensemble for the residues in the N-terminal helix. As reported earlier (Santoro et al., 1993), exchange rates for backbone N−H's for the residues in the N-terminal helix were all in the fastest-exchange group (>1.5 x 10^{-2} min^{-1}; Figure 5 of Santoro et al., 1993), suggesting that, in solution, there is no static packing of the N-terminal helix against other portions of the globular protein.

As indicated above, under native conditions, the fluorescence decay data of the three derivatives could not be fitted satisfactorily without the inclusion of a second subpopulation which contributed (10 ± 4) % of the total area and exhibited an EED distribution comparable to that found in the unfolded state for all three derivatives (Table 4, footnote *g*, and Figure 9). However, in the present case, the chromatographic profiles (Figure 2) and the control studies showing the stability of the probes to laser excitation (see last part of section entitled ***Control Experiments and Assumptions in the Analysis***, within the Discussion section) demonstrate that this effect cannot be attributed to a fraction of derivatives lacking the acceptor probe. In principle, it is conceivable that a propagated conformational change induced by the attachment of the acceptor might arise; this could increase the lifetime of the donor independent of its concomitant reduction by energy transfer in (10 ± 4)% of the molecules. This effect is very unlikely because all three derivatives exhibited the second conformational subpopulation to the same extent. Furthermore, the enzymatic activity of the donor-only and two doubly labeled derivatives was consistently lower by 10% than the native molecule (a fourth derivative had higher activity, presumably because of specific effects at the active site of the enzyme). Therefore, we feel that the most reasonable interpretation of the available data for the N state is that a (10 ± 4)% subpopulation of unfolded molecules exists, and, given the 10% reduction in enzymatic activity relative to native of even the donor-only derivative, it appears that this phenomenon results from labeling at the C-terminus.

The Unfolded and Partially Folded States

The derivatives were examined under four separate solution conditions (defined in Materials and Methods), chosen to favor a protein chain that is (i) native-like (N); (ii) disulfide-intact and denatured (U); (iii) disulfide-reduced and denatured (R); and (iv) disulfide-reduced, but with low concentrations of denaturant (R_N). This last solution condition, R_N , was studied in order to assess conformational properties of a chain that had been transferred from strongly denaturing (6 M GdnHCl) and reducing (140 mM DTT, pH 8) conditions to folding-permissive conditions (0.6 M GdnHCl) while maintaining a reducing environment (14 mM DTT, pH 5) to prevent reformation of disulfide bonds (we designate 0.6 M GdnHCl at pH 5 as folding permissive since RNase A is >95% folded at temperatures up to 38 °C in 1 M GdnHCl, pH 4.0 (W. Houry and H. A. Scheraga, unpublished). The R_N environment should be particularly favorable for observing nonbonded interactions that may contribute to early steps in the folding pathway.

In contrast to the global analysis of the data for derivatives in the native state, the three other solution conditions for all

derivatives gave time-resolved decay data that did not show significant improvement in global χ^2 when a bimodal instead of unimodal distance distribution function was assumed for $P(r)$ (eq 5). Therefore, a single distribution of interprobe distances was assumed in all of the following discussion.

The EED of the 124-Residue Segment, (1−124) RNase A. As shown in Table 3, the transfer efficiency of (1−124)-RNase A was negligible under the three nonnative conditions studied here (0.10 in the U state and < 0.01 in the R and R_N states). This low level of donor quenching by energy transfer means that most of the interprobe distances in this derivative are greater than 1.6 times that of R_o. Interprobe distance parameters (distribution means and widths and interprobe diffusion) could not be determined with satisfactory statistical significance, except to define a lower limit of the average of the interprobe distribution separation of ca. 50 Å (Table 4). With the present pair of probes and low ET probabilities in the unfolded states, this analysis cannot show or exclude the existence of a subpopulation with a short (1−124) EED in excess of the population expected for a statistical coil. No contribution of a nonlocal interaction between the two terminal segments of the RNase A chain could be detected in the denatured and in the partially folded states of RNase A.

The 64-Residue Segment, (61−124)RNase. Unfolding of the 64-residue segment between residues 61 and 124 of (61−124)RNase A was observed upon transferring it from the N to the U state. This is reflected in a decrease in transfer efficiency, E, from 0.75 to 0.40 (Table 3) and, as shown by the global analysis in Table 4, by an increase in interprobe distribution mean from 12 to 29 Å, an increase in distribution width from $\sigma = 4.5$ to 12.2 Å, and an increase in interprobe diffusion coefficient from 0 to 1.5 Å^2/ns (Table 4, Figure 9). In the R state, following reduction of its disulfide bonds, and in the presence of denaturant, this segment was unfolded further. The negligible transfer efficiency (Table 3) meant that the parameters of the EED distribution could not be determined with satisfactory statistical confidence with the present pair of probes (Table 4).

Lowering the denaturant concentration while maintaining a reducing environment, i.e., the transition to the R_N state, caused an increase in the transfer efficiency to 0.26 (Table 3), indicating partial refolding of this segment. A very broad EED distribution (mean: 38 Å), a large width of $\sigma = 16$ Å [Table 4, Figure 9 (middle)], and a very small diffusion coefficient (< 0.5 Å^2/ns) were found. A significant fraction of the molecules had an EED of the folded state [Figure 9 (middle) in the range of 0 to 20 Å].

Two disulfide crosslinks, 58−110 and 65−72, can directly affect the distance between residues 61 and 124. With native disulfide bonds intact, the shortest path between 61 and 124 through a covalent backbone traverses the 58−110 disulfide bond and spans 19 residues *plus* the cysteinyl side chains and disulfide bond, similar to the length of the (104-124)-RNase segment (21 residues). As expected, (61−124)RNase in the U state shows similar distance parameters to those recovered for (104−124) RNase under denaturing conditions (Table 4, Figure 9).

The C-Terminal 21-Residue Segment, (104−124)RNase. Tables 3 and 4 show that the transition from the N to the U state caused an unfolding of the native, C-terminal β-sheet loop. This is reflected in a decreased E from 0.75 to 0.39, an increased distribution mean from 9.8 to 32.0 Å, an increased distribution width (σ) from 4.1 to 12.5 Å, and an increased interprobe diffusion rate from $D = 0$ to 2.9 Å^2/ns. For the R state, the recovered parameters indicate no significant change for the (104−124) segment relative to the U state.

In comparing the R_N state to the R state, a significant refolding of the C-terminal segment was observed. The transfer efficiency increased substantially to 0.56 (Table 3), the distribution mean and width (σ) decreased to 22 and 9 Å, respectively (Table 4, Figure 9), and the diffusion coefficient showed an apparent reduction to 0.5 Å^2/ns (Table 4).

This derivative was designed both to test the hypothesis that the segment forming the C-terminal antiparallel β-sheet in the native state can function as a chain folding initiation site in the early stages of folding (Matheson & Scheraga, 1978; Beals et al., 1991), and to differentiate the contributions of long- and short-range interactions in the folding of this segment. In a complementary study (Beals et al., 1991), the conformation of a model peptide analogous to the hydrophobic 105−124 C-terminal tryptic peptide of RNase-A was investigated by determination of the EED distribution under denaturing and nondenaturing conditions at different temperatures. In the previous study, Beals et al. (1991) synthesized a doubly labeled peptide corresponding to residues 105−124 of RNase A, modified by addition of 2-naphthoxyacetamide (fluorescent donor) at the N^{γ}-position of a diaminobutyric acid residue at the C-terminus, a dansyl (acceptor) group at the N-terminus (His-105), and sulfonation of the single Cys residue at position 110. In the present study, the acceptor probe is at Lys-104 and the donor was introduced by substitution of Val-124 with 2-naphthylalanine amide. Although differences exist in the exact position of the label in the two studies, they are nearly equivalent, since the chromophores in the synthetic 105−124 peptide model are separated by 20 residues plus 10 additional bonds (8 σ-bonds and 2 amide-type bonds), whereas in (104−124)-RNase A they are separated by 19 residues plus 14 additional bonds (12 σ-bonds and 2 amide; it should be noted that a single residue contributes 2 σ-bonds and 1 amide bond). Thus, the difference in separation between the probes is only a single bond length out of a total of ca. 70; therefore, a direct comparison between the parameters obtained here and those obtained from the earlier study based on positioning of probes seems reasonable. Also of concern in comparing the present and earlier study are differences in pH (pH 8 was used in the earlier study to enhance peptide solubility, whereas pH 5 was used in the present study to avoid thiol oxidation), and the incorporation of the S-sulfo group at Cys-110 to minimize its reactivity in the model peptide study. With these differences in mind, a comparison of the two studies was expected to allow further differentiation between the role of local and nonlocal interactions in promoting transitions between conformational states.

Under strongly denaturing conditions (6 M GdnHCl, 20 °C), the conformation of the model peptide as assessed by ET and global analysis of time-resolved decay data gave values for the mean and the width (σ) of the EED distribution of 37 Å and 14 Å, respectively (see Table 4 of Beals et al., 1991). The calculated mean of the EED distribution for a statistical coil state of a peptide of the same length was estimated to be about 36−38 Å [Flory, 1969; see Kostrowicki & Scheraga, (1995), for a recent theoretical treatment of the

EED for *short* chains]. In contrast, the (104−124) segment studied here under reducing conditions and 6.7 M GdnHCl (R state) gave for the mean and the width (σ) of the interprobe distribution values of 33.3 and 14 Å, respectively (Table 4), representing a distribution with a slightly shorter average distance under denaturing conditions for the segment embedded in the whole chain relative to the isolated peptide. Under denaturing conditions, the coefficient for interprobe diffusion could not be defined precisely for the isolated peptide (Beals et al., 1991) because of higher uncertainties resulting from the shorter fluorescence lifetime (τ_D) of the donor probe used in that study; in the present study, it was determined to be $1.5 < D < 8$ Å^2/ns.

It was seen for the model peptide at 20 °C (Beals et al., 1991) that transfer from the denaturing environment to a nondenaturing one (50 mM bicine, pH 8) resulted in an increase in ordered structure, reflected in a decrease in interprobe distribution mean (37 to 34 Å) and a decrease in distribution width (σ = 14 to 7 Å). With increasing temperature, the peptide was found to undergo yet further ordering of its structure, presumably as a result of hydrophobic interactions, obtaining an EED distribution average and width of 28.5 Å and 7Å, respectively, at the highest temperature studied (60 °C). These values for the isolated peptide under nondenaturing solution conditions should be compared with the parameters obtained here for the major subpopulation found for the (104−124) derivative in the N state, giving much shorter (average = 9.8 Å) and narrower (σ = 4.1 Å) interprobe distribution parameters. In the N state, the interprobe diffusion rate for (104−124)RNase A was the lowest measured in this study, $D < 0.3$ Å^2/ns at the 98% confidence level. This comparison supports the earlier conclusion (Beals et al., 1991) that, although partially ordered, the isolated peptide in solution does not attain a stable nativelike conformation.

The conditions of the R_N state were devised to favor the weak intrachain interactions, both local and nonlocal, while preventing formation of disulfide bonds. Both the model peptide and the C-terminal segment are considerably folded under these conditions. The C-terminal segment in the presence of the whole chain was examined under conditions (presence of 0.6 M GdnHCl) that are less stabilizing for the folded state than those used in the model peptide study (absence of GdnHCl), yet the mean of the interprobe distribution was 12 Å shorter for the (104−124) segment than for the isolated peptide. The observed EED distribution parameters for both the model peptide and the (104−124) segment in the R_N state are not consistent with a statistical coil conformation (expected EED average, 36−38 Å). Further, in comparison with the denatured states, there is a significant reduction in the interprobe diffusion rate in the R_N state to $D = 0.5$ Å^2/ns (Table 4), close to the low diffusion rate seen in the native state, and lower than the high values (2.9 and 4.7 Å^2/ns in the U and R states, respectively), also indicating formation of ordered conformations. On the other hand, average distances in both cases are significantly different from those expected for either a 21-residue helix (ca. 33 Å) or for a native antiparallel β-sheet (ca. 6 Å). Thus, it appears that the conformation of the 104−124 segment in the protein in 0.6 M GdnHCl is more ordered than the model peptide in the absence of denaturant. If the difference in pH or presence of the S-sulfo group for the peptide is not the origin of this difference, then we must conclude that, under partially folding conditions, there are *nonlocal interactions between segments of the RNase A chain that stabilize limited local folding in the C-terminal segment.*

CONCLUSIONS

The study presented here has demonstrated an application of site-specific chemical modification of a polypeptide to study its conformational properties relevant to protein folding. The labeled derivatives were determined to be suitable for folding studies since all retained enzymatic activity and the donor-only derivative was confirmed to undergo a reversible thermal unfolding/folding transition.

In this study, intramolecular diffusion coefficients between the sites labeled by the probes were obtained with improved confidence ranges compared to previous studies (Beals et al., 1991; Gottfried & Haas, 1992) by the use of a donor probe with a long fluorescence lifetime. *The intramolecular segmental diffusion coefficient was effective in determining dynamic flexibility of segments of the chain.* Clearly, the addition of conformational restrictions by the local and nonlocal interactions reduce the fluctuations.

The conformation of the labeled RNase A derivatives in the native state was different from the structure determined by crystallography in two respects: the N-terminal segment is flexible, and there is a subpopulation of (10 ± 4)% of molecules mostly unfolded. The available relative enzymatic activity data suggest that the presence of this unfolded population in the present samples may have resulted from modification at the C-terminus. Further investigation is required to clarify this point.

The measurements show that the denatured state and the partially folded states are far from being properly described as statistical coils (Chavez & Scheraga, 1980b), and an assessment of the contributions of both local and nonlocal interactions has been attempted by comparison of the present results with our earlier study using a model peptide of the C-terminal region (Beals et al., 1991).

This study shows that the C-terminal segment of the RNase A molecule has a structure even in the unfolded state. This structure is not the native structure. The structure is stabilized by local and nonlocal interactions and may well be an early CFIS (Matheson & Scheraga, 1978). Kinetic experiments are needed in order to address the question of the temporal order of action of the local and nonlocal interactions.

The current experiments again show the effectiveness of the long-range distance determination for investigating the structure and flexibility of the early folding intermediates and of the functional native state.

ACKNOWLEDGMENT

We thank T. W. Thannhauser for mass spectroscopic and R. W. Sherwood for amino acid analyses, performed at the Cornell Biotechnology Center, and V. G. Davenport, D. Friedman, L. Varshavsky, and S. E. Zimmerman for excellent technical assistance with spectroscopic measurements. D. M. Rothwarf, G. Haran, W. A. Houry, R. Dodge, S. Talluri, and R. W. Ashton provided invaluable comments and advice. Finally, we thank V. Ittah for advice and assistance in the time-resolved measurements and data analyses.

REFERENCES

Amir, D., & Haas, E. (1987) *Biochemistry 26*, 2162−2175.

Amir, D., Krausz, S., & Haas, E. (1992) *Proteins: Struct., Funct., Genet. 13*, 162−173.
Beals, J. M., Haas, E., Krausz, S., & Scheraga, H. A. (1991) *Biochemistry 30*, 7680−7692.
Beechem, J. M., & Haas, E. (1989) *Biophys J. 55*, 1225−1236.
Buckler, D. R., Haas, E., & Scheraga, H. A. (1993) *Anal. Biochem. 209*, 20−31.
Burgess, A. W., & Scheraga, H. A. (1975) *J. Theor. Biol. 53*, 403−420.
Chavez, L. G., Jr., & Scheraga, H. A. (1980a) *Biochemistry 19*, 996−1004.
Chavez, L. G., Jr., & Scheraga, H. A. (1980b) *Biochemistry 19*, 1005−1012.
Chen, R. F., Edelhoch, H., & Steiner, R. F. (1969) in *Physical Principles and Techniques of Protein Chemistry* (Leach, S. J., Ed.) part A, pp 204−208, Academic Press, New York.
Cooke, J. P., Anfinsen, C. B., & Sela, M. (1963) *J. Biol. Chem. 238*, 2034−2039.
Crook, E. M., Mathias, A. P., Rabin, B. R. (1960) *Biochem. J. 74*, 234−238.
Dale, R. E., Eisinger, J., & Blumberg, W. E. (1979) *Biophys. J., 26*, 161−194.
Denton, J. B., Konishi, Y., & Scheraga, H. A. (1982) *Biochemistry 21*, 5155−5163.
Denton, M. E., Rothwarf, D. M., & Scheraga, H. A. (1994) *Biochemistry 33*, 11225−11236.
Flory, P. J. (1969) *Statistical Mechanics of Chain Molecules*, pp 8−9, Wiley-Interscience, New York.
Förster, Th. (1948) *Ann. Phys. (Leipzig) 2*, 55−75.
Forster, Y., & Haas, E. (1993) *Anal. Biochem. 209*, 9−14.
Fujioka, H., & Scheraga, H. A. (1965) *Biochemistry 4*, 2197−2205, 2206−2218.
Gottfried, D. S., & Haas, E. (1992) *Biochemistry 31*, 12353−12362.
Haas, E., Katchalski-Katzir, E., & Steinberg, I. Z. (1978a) *Biopolymers 17*, 11−31.
Haas, E., Katchalski-Katzir, E., & Steinberg, I. Z. (1978b) *Biochemistry 17*, 5064−5070.
Haas, E., Wilchek, M., Katchalski-Katzir, E., & Steinberg, I. Z. (1975) *Proc. Natl. Acad. Sci., U.S.A. 72*,1807−1811.
Haran, G., Haas, E. Szpikowska, B. K., & Mas, M. T. (1992) *Proc. Natl. Acad. Sci., U.S.A. 89*, 11764−11768.
Hillel, Z., & Wu, C. W. (1976) *Biochemistry 15*, 2105−2113.
Ittah, V., & Haas, E. (1995). *Biochemistry 34*, 4493−4506.
Jones, R. E. (1970) *Nanoseconds Fluorimetry*, Ph.D. Thesis, Stanford University.
Kirby, E. P., & Steiner, R. F. (1970) *J. Phys. Chem. 74*, 4480−4490.
Kostrowicki, J., & Scheraga, H. A. (1995) *Comput. Polym. Sci. 5*, 47−55.
Matheson, R. R., Jr., & Scheraga, H. A. (1978) *Macromolecules 11*, 819−829.
McWherter, C. A.,. Haas, E., Leed, A. R., & Scheraga, H. A. (1986) *Biochemistry 25*, 1951−1963.
Montelione, G. T., & Scheraga, H. A. (1989) *Acc. Chem. Res. 22*, 70−76.
Richards, F. M., & Wyckoff, H. W. (1971) in *The Enzymes* (Boyer, P. D. Ed.) 3rd ed., Vol. IV, pp 647−806, *Academic Press*, New York.
Santoro, J. Gonzales, C., Bruix, M., Neira, J. L., Nieto, J. L., Herranz, J., & Rico, M. (1993) *J. Mol. Biol. 229*, 722−734.
Shinitzky, M. (1972) *J. Chem. Phys. 56*, 5979−5981.
Stryer, L. (1978) *Annu. Rev. Biochem. 47*, 819−846.
Wlodawer, A., Svensson, L. A, Sjölin, L. A., & Gilliland, G. L. (1988). *Biochemistry 27*, 2705−2717.
Wright, P. E., Dyson, H. J., & Lerner, R. A. (1988) *Biochemistry 27*, 7167−7175.
Wu, P., & Brand, L. (1992) *Biochemistry 31*, 7939−7947.

BI950745V